Int. J. Solids Structures, 1975, Vol. 11, pp. 1–19. Pergamon Press. Printed in Gt. Britain.

PLASTIC AND VISCOPLASTIC ANALYSIS OF AXISYMMETRIC SHELLS

S. NAGARAJAN† and E. P. POPOV‡
University of California, Berkeley, California 94720, U.S.A.

(*Received* 31 *December* 1973; *revised* 21 *February* 1974)

Abstract—A general formulation of large deformation analysis of plastic and viscoplastic problems is presented first. The equilibrium equations are derived from an incremental variational formulation using the Lagrangian mode of description of motion. The symmetric Piola–Kirchhoff stress and Lagrangian strain are used in all the constitutive relations. Using degenerate isoparametric elements, permitting relaxation of the Kirchhoff–Love hypothesis, the procedure is specialized for the finite element analysis of shells of revolution subjected to axisymmetric loading. A modified incremental method, which applies an equilibrium correction at each step, is used for the solution of the linearized incremental equilibrium equations. Two approaches are presented for adapting the viscoplasticity formulation to provide inviscid plasticity solutions—one involving the extrapolation of results as the viscosity coefficient tends to infinity, and the other in which plasticity solutions are obtained by using time as an artifice in the viscoplastic analysis until equilibrium states are achieved at each succeeding load level. A detailed study of the nonlinear behavior of a torispherical pressure vessel is presented to illustrate the effectiveness of the numerical techniques.

1. INTRODUCTION

The finite element method has been used successfully in recent years in the development of efficient numerical techniques for the nonlinear analysis of deformable bodies. Several authors have considered the combined effect of material and geometric nonlinearities, notable among these being Marcal[1], Yaghmai[2], Hofmeister *et al.*[3] and Larsen[4]. However, very little attention has been paid to the study of practical problems involving rate dependent deformations. The classical inviscid plasticity theory is inadequate for dealing with such problems and recourse must be made to theories reflecting strain rate sensitivity. Constitutive laws have been proposed by several authors for rate sensitive materials. These have been summarized and discussed by Perzyna[5], Lindholm[6] and Cristescu[7]. Although many experimental studies have been reported[8–12], application of finite element methods to this class of viscoplastic problems is lagging far behind and literature in this field is almost nonexistent, except for the work of Zienkiewicz and Cormeau[13] which studies some simple problems.

A general formulation is presented herein for the large deformation analysis of plastic and viscoplastic problems. Virtual work expressions written using the Lagrangian mode of description of motion lead to the incremental equilibrium equations. The classical inviscid theory of plasticity using von Mises yield criterion as well as the viscoplastic laws taking into account strain rate dependent deformations are both considered. While the tangent stiffness method is used to treat elastic–plastic problems, an initial strain approach is used to

† Assistant Research Engineer.
‡ Professor of Civil Engineering.

take into account viscoplastic material behavior. The finite element idealization is based on the degenerate isoparametric elements, permitting relaxation of the Kirchhoff–Love Hypothesis, and the numerical method presented is specialized for the analysis of shells of revolution under axisymmetric loading. An equilibrium correction is used at each step to improve the accuracy of the incremental solution procedure. The nonlinear behavior of a torispherical pressure head subjected to uniform internal pressure is studied and elastic–plastic as well as elastic–viscoplastic solutions are presented to demonstrate the effectiveness of the numerical techniques. The procedures for obtaining elastic-plastic solutions using the viscoplasticity formulation are also shown to yield very good results.

2. KINEMATICS

The path of deformation of a three-dimensional body may be described by considering the three configurations shown in Fig. 1. The initial configuration is denoted by B_0, the current by B_1, and a neighboring configuration to B_1 is indicated by B_2. A fixed, orthogonal curvilinear coordinate system with coordinates x^I and base vectors $\mathbf{G}_I$ is associated with configuration B_0, while B_1 is described by x^i and $\mathbf{g}_i$, and B_2 by $\bar{X}^\alpha$ and $\bar{g}_\alpha$, all the indices having the range 1 to 3. The coordinate system X^I will be assumed to be a global system in which the motion is described.

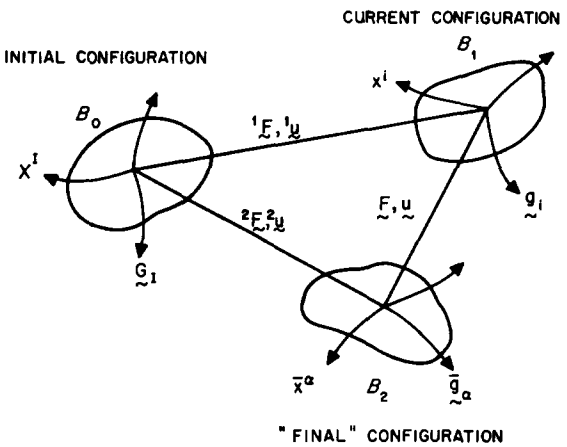

Fig. 1. Description of motion—Configurations of a body in its path of deformation.

The position of a generic material point in B_0, B_1 and B_2 is described by $\mathbf{X}$, $\mathbf{x}$ and $\bar{\mathbf{x}}$, respectively, where

$$\mathbf{x} = \mathbf{X} + {}^1\mathbf{u} \tag{1a}$$

$$\bar{\mathbf{x}} = \mathbf{X} + {}^2\mathbf{u} = \mathbf{x} + {}^2\mathbf{u} - {}^1\mathbf{u} = \mathbf{x} + \mathbf{u}. \tag{1b}$$

Here ${}^2\mathbf{u}$ and ${}^1\mathbf{u}$ are the total displacement vectors in B_2 and B_1, respectively, and $\mathbf{u}$ the incremental displacement from B_1 to B_2. In this notation, the Lagrangian strain in B_1 is defined† as

$$2\,{}^1E_{IJ} = {}^1u_{I,J} + {}^1u_{J,I} + {}^1u_{K,I}\,{}^1u_{K,J}. \tag{2a}$$

† For the sake of simplicity, rectangular Cartesian coordinates are used when component forms are written; capital indices indicate that components are relative to B_0.

Similarly, the Lagrangian strain in B_2 can be written as

$$2^2E_{IJ} = {}^2u_{I,J} + {}^2u_{J,I} + {}^2u_{K,I}\,{}^2u_{K,J}. \tag{2b}$$

The strain increment from B_1 to B_2, referred to the initial configuration B_0, is obtained simply as

$$2E_{IJ} = 2({}^2E_{IJ} - {}^1E_{IJ}) \tag{3}$$

Substituting Equations (2a, 2b) into (3), and using the relation ${}^2\mathbf{u} = {}^1\mathbf{u} + \mathbf{u}$ from (1b), one can get

$$2E_{IJ} = u_{I,J} + u_{J,I} + {}^1u_{K,}u_{K,IJ} + u_{K,I}\,{}^1u_{K,J} + u_{K,I}u_{K,J}. \tag{4}$$

The strain increment E_{IJ} may be decomposed into

$$E_{IJ} = e_{IJ} + \eta_{IJ} \tag{5}$$

where e_{IJ} and η_{IJ} are the linear and nonlinear parts, respectively, and are defined as

$$2e_{IJ} = u_{I,J} + u_{J,I} + {}^1u_{K,}u_{K,JI} + u_{K,I}\,{}^1u_{K,J} \tag{6a}$$

$$2\eta_{IJ} = u_{K,}\,{}^1u_{K,J}. \tag{6b}$$

3. INCREMENTAL EQUILIBRIUM EQUATIONS

The incremental equations of equilibrium are derived by taking the difference between the virtual work expressions in configurations B_2 and B_1 written with respect to a common reference state. The Lagrangian mode of description of motion is used in this paper, and involves the use of initial configuration B_0 as the reference state. The details of derivation may be found in Refs.[14–16]. Neglecting inertia and body forces, the incremental virtual work expression may be written as[16]

$$\int_{B_0} (S_{IJ}\,\delta E_{IJ} + {}^1S_{IJ}\,\delta\eta_{IJ})\,\mathrm{d}V = \int_{\partial B_2} \delta u_I\,{}^2t_I\,\mathrm{d}\bar{a} - \int_{\partial B_1} \delta u_I\,{}^1t_I\,\mathrm{d}a \tag{7}$$

where ${}^1\mathbf{t}$, ${}^2\mathbf{t}$ are traction vectors in B_1 and B_2, respectively, and ∂B_i refers to the surface of B_i where surface tractions are specified. $\mathrm{d}V$ is the volume element in B_0, $\mathrm{d}a$, $\mathrm{d}v$ are the infinitesimal surface and volume elements in B_1, and the equivalent elements in B_2 are denoted by $\mathrm{d}\bar{a}$, $\mathrm{d}\bar{v}$. The increment in the symmetric Piola–Kirchhoff stress tensor is defined as $\mathbf{S} = {}^2\mathbf{S} - {}^1\mathbf{S}$ and obtained in terms of $\mathbf{E}$ through a linear transformation tensor $\mathbf{C}$, i.e.

$$\mathbf{S} = \mathbf{CE}. \tag{8}$$

Since $\mathbf{S}$ is nonlinear in $\mathbf{u}$, substitution of Equation (8) into (7) results in nonlinear equilibrium equations. A linearized form of (7) is obtained when $\mathbf{E}$ is replaced by $\mathbf{e}$ in (8). The internal stress field obtained using the linearized equations does not necessarily equilibrate the applied loading. The out-of-balance force may be accounted for, and improved convergence obtained, by adding a residual loading term to the right-hand side of Equation (7) which then becomes

$$\int_{B_0} (S_{IJ}\,\delta e_{IJ} + {}^1S_{IJ}\,\delta\eta_{IJ})\,\mathrm{d}V = \int_{\partial B_2} \delta u_I\,{}^2t_I\,\mathrm{d}\bar{a} - \int_{B_0}^{1} S_{IJ}\,\delta e_{IJ}\,\mathrm{d}V \tag{9}$$

where the second integral on the right-hand side represents the force which equilibrates the internal stress field. In the displacement formulation of the finite element method, the left-hand side gives rise to the well-known incremental and geometric stiffness matrices.

The first integral on the right-hand side represents the applied loading in configuration B_2. This integral must be transformed from ∂B_2 to ∂B_0 and specialized for the cases of conservative and nonconservative loading. This problem has been discussed earlier [16–18]. Assuming the displacement increments $\mathbf{u}$ to be small compared to ${}^1\mathbf{u}$, and the rotations associated with $\mathbf{u}$ to be small compared to unity, this integral is transformed[16] for nonconservative loading of the pressure type into

$$\int_{\partial B_0} \frac{\rho_0}{\rho} {}^2p \, \delta u_I \left(\frac{\partial X_J}{\partial x_I} - \frac{\partial X_J}{\partial x_K} \frac{\partial X_M}{\partial x_J} \frac{\partial u_K}{\partial X_M} \right) N_J \, \mathrm{d}A \tag{10a}$$

and for conservative loading into

$$\int_{\partial B_0} \delta u_I {}^2\bar{t}_J \left(\frac{\partial X_J}{\partial x_I} - \frac{\partial X_J}{\partial x_K} \frac{\partial X_M}{\partial x_J} \frac{\partial u_K}{\partial X_M} \right) \mathrm{d}A \tag{10b}$$

Here ${}^2p$ is the pressure on a surface element in B_2 and ${}^2\bar{t}_J$ the components of ${}^2\bar{t}$, the traction vector in B_2 measured per unit area in B_0, relative to the convected base vectors in B_2. The second terms in the parentheses of the two expressions are linear in $\mathbf{u}$ and give rise to additional stiffness terms which are nonsymmetric. For most engineering applications, the norms of these terms are small compared to the norms of the stiffness terms in Equation (9). Hence their effect on the total stiffness of the system is small and they are neglected from further consideration, especially in view of the significant additional computational effort needed to solve a set of equations with nonsymmetric coefficient matrix.

3.1 *Modification of virtual work expression for viscoplasticity*

The application of the incremental virtual work expression of equation (7) for viscoplastic material behavior is based on the following assumptions:

(i) The additive decomposition law is valid for the Lagrangian strain rate tensor, i.e.

$$\dot{E}_{IJ} = \dot{E}^I_{IJ} + \dot{E}^{vp}_{IJ} \tag{11}$$

where $\dot{E}^I_{IJ}$, the instantaneous strain rate, and $\dot{E}^{vp}_{IJ}$, the viscoplastic strain rate, are assumed to be defined by constitutive relations and not given kinematic interpretation. For sufficiently small time steps, a similar equation is valid for strain increments. Although additive decomposition of strain rates is not the only method of decomposing kinematic variables, it is the most convenient form for use in a Lagrangian description. A comparative discussion of the many different approaches toward the kinematic decomposition of finite inelastic deformations has been presented by Larsen[4, 19].

(ii) There exists a linear relationship between the increment of Piola–Kirchhoff stress and the instantaneous strain increment, i.e.

$$S_{IJ} = C_{IJKL} E^I_{KL}. \tag{12}$$

The instantaneous strain increment E^I_{IJ} equals the elastic strain increment E^E_{IJ} in the case of viscoplasticity. E^{vp}_{IJ} vanishes for problems in classical inviscid plasticity wherein the increment in instantaneous strain rate is decomposed into elastic and plastic components, i.e.

$$\dot{E}_{IJ} = \dot{E}^I_{IJ} = \dot{E}^E_{IJ} + \dot{E}^p_{IJ}. \tag{13}$$

The viscoplastic strain rate is assumed to be independent of the stress rate and the viscoplastic strain increments are taken into account in the equilibrium equations in terms of an initial strain formulation. Combining equations (11, 12) gives

$$S_{IJ} = C_{IJKL}(E_{KL} - E^{VP}_{KL}) = S^{I}_{IJ} - S^{VP}_{IJ} \tag{14a}$$

where

$$S^{I}_{IJ} = C_{IJKL}E_{KL},\ S^{VL}_{KL} = C_{IJKL}E^{VP}_{KL} \tag{14b}$$

may be defined as the instantaneous and viscoplastic stress increments, respectively, and possess the same invariance properties as S_{IJ}. The incremental virtual work due to the internal stress field may then be modified by the substitution of equation (14a) for the stress increment S_{IJ} into the left-hand side of equation (7), i.e.

$$\delta W_2 - \delta W_1 = \int_{B_0} [S^{I}_{IJ}\delta E_{IJ} + ({}^{1}S_{IJ} - S^{VP}_{IJ})\delta\eta_{IJ} - S^{VP}_{IJ}\delta e_{IJ}]\,\mathrm{d}V. \tag{15a}$$

It can be seen from equation (15a) that a viscoplastic pseudo-loading term as well as a contribution to the geometric stiffness arise as a result of consideration of the viscoplastic strain in the formulation. If the linearized form given in equation (9) is used instead of (7), one obtains

$$\delta X_2 - \delta W_1 = \int_{B_0} [S^{I}_{IJ}\delta e_{IJ} + {}^{1}S_{IJ}\,\delta\eta_{IJ} - S^{VP}_{IJ}\,\delta e_{IJ}]\,\mathrm{d}V \tag{15b}$$

which exhibits only the viscoplastic pseudo-loading term as a result of the initial strain.

4. INCREMENTAL CONSTITUTIVE RELATIONS

The incremental expression of virtual work given in equation (9) is not restricted to any particular constitutive laws of material behavior. The next step in the theoretical formulation is to obtain incremental constitutive laws in terms of the Lagrangian strain tensor and the 2nd Piola–Kirchhoff stress tensor to be used in conjunction with the virtual work expression.

4.1 *Elasticity*

The incremental constitutive equations for an elastic continuum are well known and take the form

$$S_{IJ} = C_{IJKL}E_{KL} \tag{16}$$

where the stress–strain transformation tensor for isotropic, linear elastic materials is given by

$$C_{IJKL} = E_{IJKL} = \mu(\delta_{IK}\delta_{JL} + \delta_{IL}\delta_{JK}) + \lambda\delta_{IJ}\delta_{KL} \tag{17}$$

with λ and μ being the Lamé constants.

4.2 *Plasticity*

The incremental theory of plasticity, using the associated flow rule with von Mises yield condition and isotropic hardening, is adopted in this paper as the basis for establishing the constitutive equations for plastic strain increments. The extension of the infinitesimal theory of plasticity to the special case of small strains, large rotations is based on the use of the 2nd Piola–Kirchhoff stress and the postulate that the physical components of the Cauchy stress tensor in surface coordinates of the deformed shell are approximately equal

to the components of the P–K stress in the undeformed configuration[4]. It follows from this that the mathematical representation of the yield function is the same in both the Cauchy and P–K stress spaces.

For an initially isotropic material, the von Mises yield condition in the current configuration B_1 is expressed as

$$F({}^1S_{IJ}) = F(J_2) = J_2 = k^2 \tag{18a}$$

or

$$f = J_2 - k^2 = 0 \tag{18b}$$

where the yield function depends on J_2, the second invariant of the deviatoric stress tensor ${}^1\bar{S}_{IJ}$, and k, the yield stress in pure shear. Using isotropic hardening, the subsequent yield surfaces can be written as

$$f = F({}^1S_{IJ}) - H({}^1E^P_{IJ}) = 0 \tag{19}$$

where H is a hardening parameter. This parameter may also be expressed in terms of the strain hardening parameter[20] which can be determined from uniaxial tension test.

Following[20], it is possible to obtain an expression for the incremental plastic strains in terms of the increments in total strains by combining the associated flow rule

$${}^1\dot{E}^P_{IJ} = \mathbf{y}\frac{\partial f}{\partial {}^1S_{IJ}}\ ;\ \dot{\lambda} \text{ a non-negative scalar,} \tag{20a}$$

the consistency condition

$$\mathrm{d}f = \frac{\partial p}{\partial {}^1S_{IJ}} S_{IJ} + \frac{\partial f}{\partial {}^1E^P_{IJ}} E^P_{IJ} = 0 \tag{20b}$$

and the generalized Hooke's law

$$S_{IJ} = E_{IJKL}E^E_{KL} = E_{IJKL}(E_{KL} - E^P_{KL}). \tag{20c}$$

The resulting equation has the form

$$E^P_{IJ} = A_{IJKL}E_{KL} \tag{21a}$$

where the transformation tensor A_{IJKL} is given by

$$A_{IJKL} = h\frac{\partial f}{\partial {}^1S_{IJ}}\frac{\partial f}{\partial {}^1S_{MN}}E_{MNKL} \tag{21b}$$

and

$$h^{-1} = \frac{\partial f}{\partial {}^1S_{IJ}}\frac{\partial f}{\partial {}^1S_{KL}}E_{IJKL} - \frac{\partial f}{\partial {}^1S_{IJ}}\frac{\partial f}{\partial {}^1E^P_{IJ}}, \tag{21c}$$

Finally, substituting equation (21a) into (20c), the incremental stress–strain law is obtained as

$$S_{IJ} = C_{IJKL}E_{KL} \tag{22a}$$

where

$$C_{IJKL} = E_{IJKL} - E_{IJMN}A_{MNKL}. \tag{22b}$$

For von Mises yield condition and isotropic hardening, the expressions in equations (21b, 22b) can be simplified to

$$A_{IJKL} = (9\mu h/2\bar{\sigma}^2)^1\bar{S}_{IJ}{}^1\bar{S}_{KL} \tag{23}$$

and

$$C_{IJKL} = \mu(\delta_{IK}\delta_{JL} = \delta_{1L}\delta_{JK}) + \lambda\delta_{IJ}\delta_{KL} - 9^{\mu 2}h^1\bar{S}_{IJ}{}^1\bar{S}_{KL}/\bar{\sigma}^2 \tag{24}$$

where $h = \dfrac{2(1+\nu)(1-\zeta)}{E[3-\zeta(1-2\nu)]}$, $\zeta = E_t/E$, and $\bar{\sigma} = \sqrt{3J_2}$, the equivalent stress.

In addition to the constitutive relations, it is also necessary to define a loading/unloading criterion. Depending on the state of stress, the yield function f is computed and an elastic state is indicated if $f < 0$ and a plastic state if $f = 0$; $f > 0$ constitutes an inadmissible state in the theory of plasticity. Associated with the plastic state $f = 0$, three types of behavior are recognized, viz. loading, unloading and neutral loading which are characterized by $\dot{f} > 0, \dot{f} < 0$ and $\dot{f} = 0$, respectively.

4.3 *Viscoplasticity*

The uniaxial behavior of a viscoplastic material was described by Malvern[21] in terms of a reference static stress–strain function. The viscoplastic strain rate was considered to be proportional to the excess stress above this reference, the proportionality factor being a function of the material viscosity. Lubliner[22] proposed a squasilinear differential form of constitutive equation that contained as special cases the rate-dependent theories of Sokolovsky[23] and Malvern[21], as well as the rate-independent theories of van Karman[24] Rakhmatulin[25], and Taylor[26]. Also Lubliner modified Malvern's theory by imposing a limiting maximum dynamic stress–strain curve. Perzyna[27] gave a multiaxial form of Malvern's law by the generalization of a more restricted viscoplastic law introduced by Hohenemeser and Prager[28]. Perzyna and Wojno[29] extended the multiaxial theory to finite strains. The basic assumption of all these theories is that viscoplastic deformations occur only when a certain threshold static yield surface is exceeded and below which the response is purely elastic. Linearized versions of these viscoplastic laws have been used for the analytical solution of some simple cases[30, 31], but more complex problems may be considered by the use of numerical techniques such as the finite element methods.

Following Perzyna, the viscoplastic strain rate is assumed to be given by

$${}^1\dot{E}_{IJ}^{VP} = \bar{\gamma} < \Phi(\mathscr{F}) > \frac{\partial F}{\partial {}^1S_{IJ}} \tag{25}$$

where $\bar{\gamma}$ is a material viscosity co-efficient, and $\mathscr{F}$ a scalar yield function. In terms of the static loading surface, equation (19), the function $\mathscr{F}$ is expressed as

$$\mathscr{F} = \frac{F({}^1S_{IJ}) - H({}^1E_{IJ}^{VP})}{NH({}^1E_{IJ}^{VP})} = \frac{f}{H}. \tag{26}$$

The expression for the viscoplastic strain rate, equation (25), assumes that the material obeys the von Mises yield criterion with isotropic hardening and associated flow rule for static deformations, and equation (26) implies that the visco–plastic strain rate depends on the amount by which the static loading surface is exceeded. The notation $< >$ in equation (25)

means that

$$\langle \Phi(\mathscr{F}) \rangle = \begin{cases} \Phi(\mathscr{F}) & \text{when } \Phi(\mathscr{F}) > 0 \\ 0 & \text{when } \Phi(\mathscr{F}) \leq 0. \end{cases} \tag{27}$$

In other words, viscoplastic deformation occurs only when $\Phi(\mathscr{F})$ exceeds zero. Different functional forms have been proposed[32] for Φ to describe the process and the simplest form is chosen in this study, viz.

$$\Phi(\mathscr{F}) = \mathscr{F}. \tag{28}$$

It should be noted that $\mathscr{F} > 0$ constitutes an inadmissible state in the theory of inviscid plasticity (the plastic state being identified by $\mathscr{F} = 0$) but in viscoplasticity $\mathscr{F} > 0$ is admissible and indicates viscoplastic flow. Using equations (26, 28) in (25) and introducing the expression[20], $\dfrac{\partial F}{\partial {}^1S_{IJ}} = \dfrac{3\,{}^1\bar{S}_{IJ}}{2\sqrt{3J_2}}$, for the partial derivative, one obtains

$${}^1\dot{E}^{VP}_{IJ} = \bar{\gamma}\left(\frac{\sqrt{3J_2} - H}{H}\right)\frac{3\,{}^1\bar{S}_{IJ}}{2\sqrt{3J_2}} = \frac{\sqrt{3}}{2}\frac{\bar{\gamma}}{H/\sqrt{3}}\left(\frac{\sqrt{3J_2} - H}{\sqrt{3J_2}}\right){}^1\bar{S}_{IJ}$$

or,

$${}^1\dot{E}^{VP}_{IJ} = \begin{cases} \dfrac{\gamma}{H/\sqrt{3}}\left(1 - \dfrac{H}{\sqrt{3J_2}}\right){}^1\bar{S}_{IJ} & \text{when } \dfrac{\sqrt{3J_2}}{H} - 1 > 0 \\ 0 & \text{when } \dfrac{\sqrt{3J_2}}{H} - 1 \leq 0 \end{cases} \tag{29}$$

where $\gamma = \dfrac{\sqrt{3}}{2}\bar{\lambda}$.

A dynamic yield criterion can be obtained by squaring both sides of equation (29).

$${}^1\dot{E}^{VP}_{IJ}\,{}^1\dot{E}^{VP}_{IJ} = \frac{\gamma^2}{H^2/3}\left(1 - \frac{H}{\sqrt{3J_2}}\right)^2 {}^1\bar{S}_{IJ}\,{}^1\bar{S}_{IJ}$$

or

$$I_2 = \frac{\gamma^2}{H^2/3}\left(1 - \frac{H}{\sqrt{3J_2}}\right)^2 J_2$$

and

$$\sqrt{I_2} = \frac{\gamma}{H}(\sqrt{3J_2} - H) = \mathscr{F}\gamma \tag{30}$$

or

$$\sqrt{3J_2} = \frac{\gamma}{H}\sqrt{I_2} + H = H\left(\frac{\sqrt{I_2}}{\gamma} + 1\right) \tag{31}$$

where I_2 is the second invariant of the viscoplastic strain rate tensor, and equation (31)

represents and expanded yield condition for rate-sensitive materials. It is clear that as $\gamma \to \infty$, equation (31) reverts back to the static von Mises yield condition. Equation (29) can now be written as

$$ {}^{1}\dot{E}_{IJ}^{VP} = \frac{\gamma}{H/\sqrt{3}} \left(\frac{\sqrt{I_2}/\gamma}{1 + \sqrt{I_2}/\gamma} \right) {}^{1}\bar{S}_{IJ} \tag{32} $$

Since from equation (30) $\sqrt{I_2} = \mathscr{F}\gamma$, one gets

$$ {}^{1}\dot{E}_{IJ}^{VP} = \frac{\gamma}{H/\sqrt{3}} \left(\frac{\mathscr{F}}{1 + \mathscr{F}} \right) {}^{1}\bar{S}_{IJ} \tag{33} $$

Again, as $\gamma \to \infty$, it is seen from equation (32) that these equations represent inviscid plasticity with $\dot{\lambda} = \sqrt{3I_2}/H$. Thus the usefulness of this viscoplastic model is not limited to rate-sensitive behavior alone but can also be taken advantage of to obtain elastic–plastic solutions for quasi static cases. An alternative procedure towards this same end is presented in Section 4.3.1 and both methods are demonstrated in the numerical example.

The computational scheme for viscoplastic analyses can now be described. Each load increment applied on the body produces an instantaneous elastic strain, and the corresponding stress increment can be computed as

$$ S_{IJ}^{I} = S_{IJ}^{E} = E_{IJKL} E_{KL} \tag{34} $$

This increment is added to the total stress and the scalar function $\mathscr{F}$ is computed. If $\mathscr{F} \leq 0$ no viscoplastic deformations occur. If $\mathscr{F} > 0$ the viscoplastic strain rates are computed as per equation (33), and the increments in viscoplastic strains, for sufficiently small time increments, are simply

$$ E_{IJ}^{VP} = {}^{1}\dot{E}_{IJ}^{VP}\, dt. \tag{35} $$

The total equivalent viscoplastic strain is computed and the new value of H, the hardening parameter, is found using the uniaxial static stress–strain curve. The viscoplastic stresses are computed as

$$ S_{IJ}^{VP} = E_{IJKL} E_{KL}^{VP} \tag{36} $$

and the stress increments can be written as (see equation 14a)

$$ S_{IJ} = S_{IJ}^{I} - S_{IJ}^{V} = S_{IJ}^{EP} - S_{IJ}^{VP} \tag{37} $$

and the total stresses are

$$ {}^{2}S_{IJ} = {}^{1}S_{IJ} + S_{IJ}. \tag{38} $$

The viscoplastic strain increments are then treated as initial strains as discussed in Section 3.

4.3.1 *Use of viscoplasticity for plasticity solutions.* It was shown in the previous section that the viscoplasticity equations degenerate to give inviscid plasticity results as the material parameter γ tends to infinity. An alternative approach is to use any arbitrary value of γ but make use of time as an artifice and let an equilibrium plastic state, $\mathscr{F} = 0$, be attained as a result of "viscoplastic" deformations. The instantaneous response in this procedure is purely elastic and the resulting state of stress might fall outside the static yield surface, see Fig. 2. This creates the situation where $\mathscr{F} > 0$ which is inadmissible in classical

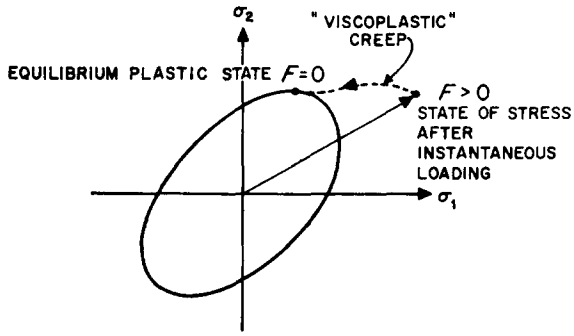

Fig. 2. "Viscoplastic" deformations leading to a steady state plasticity solution.

plasticity but not in viscoplasticity. Now, "viscoplastic" deformations are allowed to take place with time and gradually the stresses are redistributed until the state of stress at no point exceeds the yield surface, i.e. $\mathscr{F} = 0$, Fig. 2. The resulting equilibrium state is then the rate-independent elastic–plastic solution for the given problem.

5. FINITE ELEMENT ANALYSIS

The degenerate isoparametric shell element[33] is used in the present study for the finite element discretization of the structure. Rather than considering complicated kinematic relationships involved in shell theories, the element is assumed to be part of a solid, thus permitting the use of simple strain-displacement relations from three-dimensional theory of elasticity. Shear deformation is permitted in the element through relaxation of the Kirchhoff–Love hypothesis and the kinematics of the element is based on the assumption that plane sections initially normal to the middle surface remain plane, but not necessarily normal. In addition, the displacement normal to the middle surface is assumed to remain constant through the thickness.

Inclusion of shear deformation in the element permits both thin and moderately thick shells to be considered. However, special integration schemes are required[34, 35] in the case of thin shells to avoid errors arising from the existence of shear deformations in pure bending modes for the lower order elements. The excessive strain energy in shear is less important in the case of higher order elements, and an element with cubic displacement field, Fig. 3, which found successful application in axisymmetric shell analysis[4, 16], has been employed in the present study.

5.1 *Geometric representation*

The geometry of a cubic axisymmetric element, Fig. 3, is described by means of a coordinate transformation[32]

$$\begin{Bmatrix} r \\ z \end{Bmatrix} = \sum_{i=1}^{4} \phi_i(\xi) \begin{Bmatrix} r_i \\ z_i \end{Bmatrix} + \eta \sum_{i=1}^{4} \frac{1}{2} \phi_i(\xi) h_i \begin{Bmatrix} \cos\theta_i \\ \sin\theta_i \end{Bmatrix} \tag{39}$$

where $\phi_i(\xi)$ are the interpolation polynomials, h_i the thickness at node i, and θ_i the angle between the r- and η-axes as shown in Fig. 3. The local natural coordinates (ξ, η) of any point within the element are such that $-1 \leq \xi \leq +1$ and $-1 \leq \eta \leq +1$. While the ξ-axis bisects the shell thickness, the η-axis is simply defined as an axis along which $\xi = 0$. The

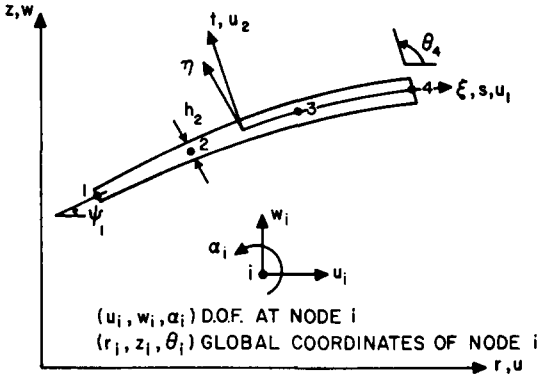

Fig. 3. Geometry of a cubic element, coordinate systems, and degrees of freedom.

outer and inner faces of the element are defined by $\eta = +1$ and $\eta = -1$, respectively. For the cubic element employed here, the nodes are located at $\xi = -1, -\frac{1}{3}, +\frac{1}{3}, +1$ and the interpolation polynomials are given by

$$\left.\begin{aligned} \phi_{1,4}(\xi) &= \frac{1}{16}(1 \mp \xi)(-1 + 9\xi^2) \\ \phi_{2,3}(\xi) &= \frac{9}{16}(1 \mp 3\xi)(1 - \xi^2) \end{aligned}\right\}. \tag{40}$$

5.2 *Displacement field*

The global displacements (u, w) at any point (ξ, η) are given by the displacement field

$$\begin{Bmatrix} u \\ w \end{Bmatrix} = \sum_{i=1}^{4} \phi_i(\xi) \begin{Bmatrix} u_i \\ w_i \end{Bmatrix} + \eta \sum_{i=1}^{4} \frac{1}{2} \phi_i(\xi) h_i \begin{Bmatrix} -\sin\theta_i \\ \cos\theta_i \end{Bmatrix} \alpha_i \tag{41}$$

which may be used for both the displacement increment $\mathbf{u}$ and the total displacement ${}^1\mathbf{u}$. The three degrees of freedom at any node i are the displacements u_i, w_i and the rotation α_i of the plane section defined by the angle θ_i, see Fig. 3. The first term in equation (41) represents the mid-surface displacement and the second term, the effect of the rotations α_i at the nodes on the global displacements at any point (ξ, η) within element.

5.3 *Strain–Displacement Matrices*

The details of the finite element formulation using degenerate isoparametric elements may be found in[4, 36] and only an outline is presented here. In a local orthogonal coordinate system (s, t), Fig. 3, the linear part of the Lagrangian strain increment between configurations B_1 and B_2 is related to the displacement gradients by means of a transformation matrix $[\Lambda]$, i.e.

$$\{e\} = [\Lambda]\{u_\delta\} \tag{42}$$

where $\{e\}^T = \langle e_{ss}\, e_{\theta\theta}\, 2e_{st} \rangle$ and $\{u_\delta\}^T = \left\langle \frac{\partial u_1}{\partial s} \frac{u}{r} \frac{\partial u_1}{\partial t} \frac{\partial u_2}{\partial s} \right\rangle$

with u_1, u_2 being the displacements relative to this local system (s, t). Recasting equation (6a) into

$$2e_{IJ} = (\delta_{KI} + {}^1u_{K,I})u_{K,J} + (\delta_{KJ} + {}^1u_{K,J})u_{K,I} \tag{43}$$

one may write an expression for $[\Lambda]$ as

$$[\Lambda] = \begin{pmatrix} \left(1 + \dfrac{\partial^1 u_1}{\partial s}\right) & 0 & 0 & \dfrac{\partial^1 u_2}{\partial s} \\ 0 & \left(1 + \dfrac{{}^1u}{r}\right) & 0 & 0 \\ \dfrac{\partial^1 u_1}{\partial t} & 0 & \left(1 + \dfrac{\partial^1 u_1}{\partial s}\right) & (1 + {}^1e_{tt}) \end{pmatrix} \tag{44}$$

where ${}^1e_{tt}$ is the physical component of normal strain computed not from kinematics but from constitutive relations condensed using the generalized plane stress conditions for axisymmetric deformations[4].

The vector of displacement gradients is obtained in terms of the displacement increment $\{u\}$ by

$$\{u_\delta\} = [B(\xi, \eta)]\{u\} \tag{45}$$

whence

$$\{e\} = [\Lambda][B]\{u\}. \tag{46}$$

The transformation matrix $[B]$ consists of gradient operators with respect to configuration B_0 and consequently remains unchanged throughout deformation history; the transformation matrix$[\Lambda]$, on the other hand, reflects the effect of prior deformations.

The nonlinear part of the strain increment, using equation (6b), is obtained as

$$\begin{Bmatrix} \eta_{ss} \\ \eta_{\theta\theta} \\ n_{st} \end{Bmatrix} = \frac{1}{2} \begin{Bmatrix} \left(\dfrac{\partial u_1}{\partial s}\right)^2 + \left(\dfrac{\partial u_2}{\partial s}\right)^2 \\ (u/r)^2 \\ \dfrac{\partial u_1}{\partial s}\dfrac{\partial u_1}{\partial t} \end{Bmatrix} \tag{47}$$

which can be represented symbolically as

$$\{\eta\} = \frac{1}{2}\{u\}^T[H]\{u\} \tag{48}$$

The matrix operator $[H]$ is composed of three submatrices, i.e.

$$[H]^T = [[H_{ss}] \vdots [H_{\theta\theta}] \vdots [H_{st}]].$$

These submatrices are given by

$$[H_{ij}(\xi, \eta)] = [B]^T[\Omega_{ij}][B]. \tag{49}$$

In this equation, $[\Omega_{ss}]$, $[\Omega_{\theta\theta}]$ and $[\Omega_{st}]$ are 4×4 matrices consisting of zero elements except

for the following elements which are unity—$[\Omega_{ss}]_{1,1 \text{ and } 4,4}$, $[\Omega_{\theta\theta}]_{2,2}$ and $[\Omega_{st}]_{1,3}$. The operator $[H]$ depends only on $[B]$ and, hence, remains unchanged through the deformation path.

5.4 *Stiffness matrices, load vectors*

The stiffness matrices and load vectors are obtained, following the methodology of the finite element method, using the linearized incremental virtual work expressions together with strain–displacement and stress–strain relations. Using equations (9, 46, 48) and neglecting the stiffness due to load (equation 10a, b), one may obtain the incremental and geometric stiffnesses, $[K_0]$ and $[K_G]$, respectively, as

$$[K_0] = 2\pi \int_{-1}^{+1} \int_{-1}^{+1} [B]^T[\Lambda]^T[C][\Lambda][B] r(\xi, \eta)\, d\eta\, d\xi \tag{50}$$

$$[K_G] = 2\pi \int_{-1}^{+1} \int_{-1}^{+1} \{{}^1S\}^T[H^{*}\quad\quad, \eta)\, d\eta\, d\xi \tag{51}$$

where

$$[H^{*T} - \quad\quad] \; \vdots \; [H_{\theta\theta}] \; \vdots \; [H_{st}] + [H_{st}]^T]$$

The applied pressure-type loading is given by

$$\{{}^2R\} = 2\pi \int_{-1}^{+1} -{}^2p \frac{\rho_0}{\rho} [{}^1F^{-1}]^T\{N\} r(\xi)\, d\xi \tag{52}$$

where $[{}^1F]$ is the matrix of deformation gradients in configuration B_1 relative to B_0, and N the vector containing components of the outward normal **N**. The internal nodal resisting forces required to equilibrate the internal stress field is

$$\{{}^1F^R\} = 2\pi \int_{-1}^{+1} \int_{-1}^{+1} [B]^T[\Lambda]^T\{{}^1S\} r(\xi, \eta)\, d\eta\, d\xi. \tag{53}$$

Finally, in the case of viscoplastic analysis, the last term in equation (15b) gives rise to additional viscoplastic pseudo-loading and is given by

$$\{R^{VP}\} = 2\pi \int_{-1}^{+1} \int_{-1}^{+1} [B]^T[\Lambda]^T\{S^{VP}\} r(\xi, \eta)\, d\eta\, d\xi \tag{54}$$

where $\{S^{VP}\}$ is the time-dependent Piola–Kirchhoff viscoplastic stress increment computed using equation (14b).

Numerical evaluation of these integrals is achieved most efficiently by carrying out the integration over the shell thickness separately. This can be achieved by proper decomposition of kinematic and stress quantities that depend on both ξ and η. While integration along the meridional direction is performed using Gaussian quadrature, it is advantageous to use Simpson integration in the transverse direction since it is capable of detecting the onset of yielding promptly in the case of elastic–plastic deformation.

6. SOLUTION METHOD

The incremental finite element equations of equilibrium are obtained as

$$([K_0] + [K_G])\{u\} = \{{}^2R\} - \{{}^1F^R\} + \{R^{VP}\}. \tag{55}$$

The equations are solved repetitively using Gaussian elimination to give a modified incremental solution that takes into account the lack of equilibrium at any step in the manner of

a one-step Newton iteration scheme. In elastic–plastic analyses the stress–strain transformation matrix $[C]$ is updated at each step for use in the computation of elastic–plastic incremental stiffness whereas the elastic stress–strain transformation $[E]$ is used throughout in viscoplastic analyses. The load at any step is specified as a fraction of the total applied load and the internal resisting force vector $\{{}^{1}F^{R}\}$ is subtracted to obtain the incremental load vector. In the case of viscoplastic analyses the load factors are given as a function of time and the incremental solution is advanced by specified time increments during each step.

The use of time in viscoplastic analyses as an artifice for obtaining elastic–plastic solutions requires the application of a number of time steps at a constant load level until an equilibrium state is reached. These time steps must be such that the viscoplastic strain increment at any point in a body is not greater than 10 to 20 per cent of the accumulated strain at any instant, failing which stability problems may arise in the solution algorithm. A possible scheme for automatic selection of time steps is presented in the work of Zienkiewicz and Cormeau[13].

7. NUMERICAL EXAMPLE

The theory presented in this paper has been applied to develop computer programs for nonlinear elastic–plastic and elastic–viscoplastic analysis of axisymmetric shells subjected to axisymmetric loads. The case of a torispherical pressure head under uniform internal pressure is taken up here to serve as an illustrative example. The shell is shown as an insert in Fig. 4 and the pertinent dimensions are indicated therein.

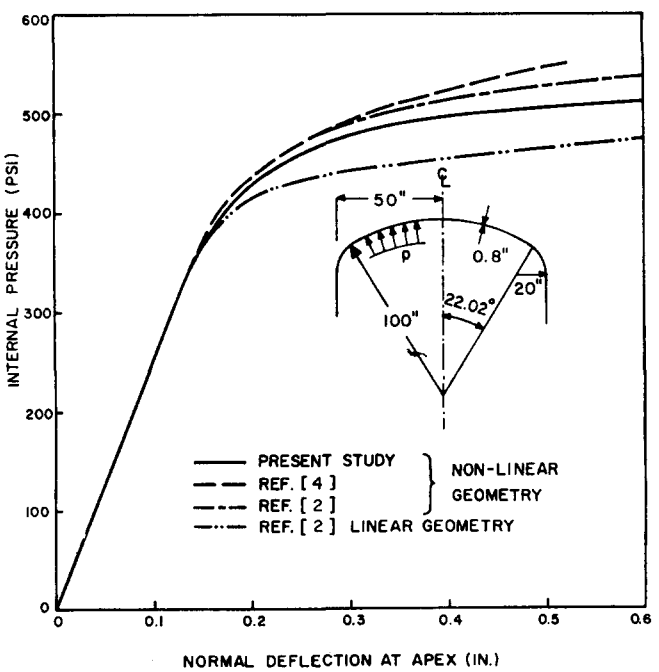

Fig. 4. Elastic–plastic analysis of torispherical pressure head.

7.1 *Elastic–plastic analysis*

The material was assumed to be elastic–perfectly plastic and to have the following properties: Young's modulus $E = 30 \times 10^6$ psi, Poisson's ratio $\nu = 0.3$, and yield stress $\sigma_y = 30{,}000$ psi. A total of 20 finite elements were used to discretize the shell from the apex to the support. Eight equal elements were used over the sphere, eight equal elements over the torus and four elements over the cylindrical portion. Four Gaussian integration points were used in the meridional direction and eleven Simpson points across the shell thickness. Very refined load increments of 5 psi were applied in the nonlinear range in order to obtain an accurate solution.

This shell was studied earlier by Yaghmai[2] using the incremental formulation based on moving reference configuration, and by Larsen[4] who used a Lagrangian formulation. The load–deflection curve for the apex displacement is plotted in Fig. 4 and compared with the results of Yaghmai ($\Delta p = 7.5$ psi) and Larsen ($\Delta p = 10$ psi). The linear solution given by Yaghmai is also plotted in the same figure. The present results indicate that the nonlinear behavior of the shell is softer than predicted in the earlier works. This is due to the use of smaller load steps which enable the softening of the system due to plasticity to be more accurately taken into account. However, the load-carrying capacity is still considerably higher than in the linear analysis and can be taken advantage of in the design of such structures.

7.2 *Elastic–viscoplastic analysis*

The elastic–viscoplastic behavior of the pressure head was studied next, assuming the same elastic–perfectly plastic material properties used earlier to represent the reference static stress–strain curve. The finite element discretization was also the same as in the case of the elastic–plastic analysis.

Solutions were obtained for four different values of the material viscosity coefficient γ (from 400 to 5000 sec^{-1}) and the internal pressure was applied at the rate of 10×10^6 psi/sec. Inertia effects were neglected but geometric nonlinearities were included in the analyses. Figure 5 shows the plots of internal pressure vs apex deflection for these viscoplastic analyses and also the elastic–plastic solution obtained in Section 7.1. It can be observed that, at lower values of γ, the viscoplastic solutions are stiff and indicate higher load-carrying capacity (tending toward elastic behavior as γ approaches zero). However, as γ increases the solution comes very close to the elastic–plastic solution, as may be expected from the discussion in Section 4.3. The two methods of obtaining elastic–plastic solutions using the viscoplasticity formulation were also pursued and the results are discussed in the following sub-section.

7.2.1 *Elastic–plastic solutions using viscoplasticity.* Elastic–viscoplastic solutions are presented in Fig. 5 for four different values of γ. Since an elastic–plastic solution is expected as $\gamma \to \infty$, a simple extrapolation procedure is used as shown in the auxiliary plots in Fig. 5. The apex displacement w is plotted as a function of $1/\gamma$ at two selected levels of internal pressure, 450 and 500 psi. For instance, the deflection at 450 psi for the four different values of γ are plotted and joined by a curve which can then be extrapolated to obtain a value of w at $1/\gamma = 0$, i.e. $\gamma = \infty$. In this case, the extrapolated curve indicates that the apex displacement at 450 psi internal pressure would be about 0.265 in. for an elastic–plastic solution. Similarly, an apex displacement of about 0.6 in. is predicted at 500 psi for an elastic–plastic pressure head. This procedure may be used to obtain the elastic–plastic apex displacement at any desired load level.

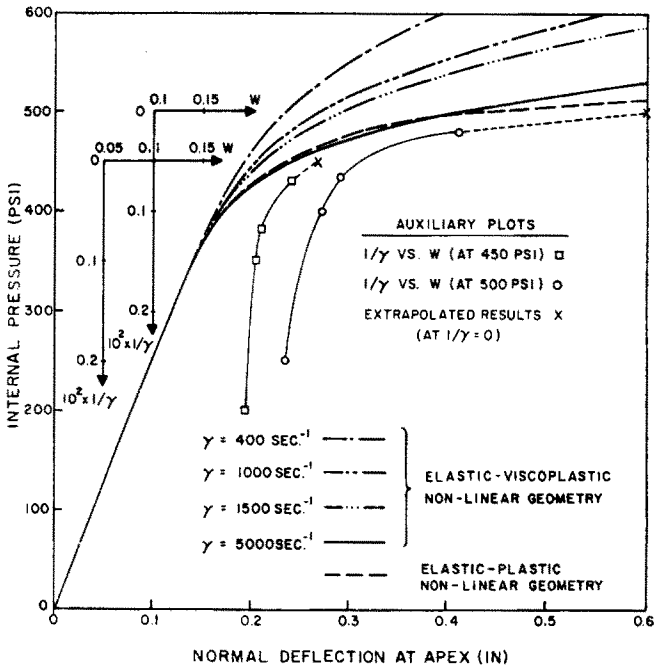

Fig. 5. Nonlinear analysis of torispherical pressure vessel under internal pressure.

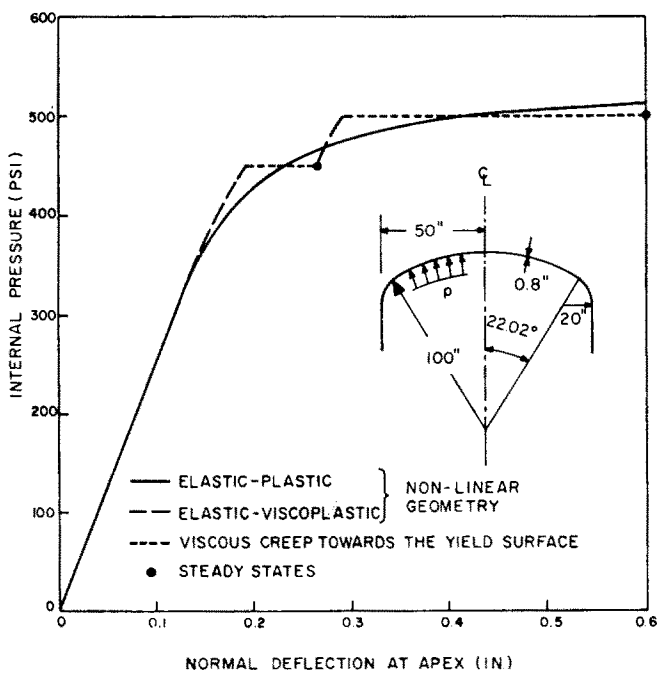

Fig. 6. Internal pressure vs. apex deflection—Elastic–plastic analysis of torispherical head using viscoplasticity formulation.

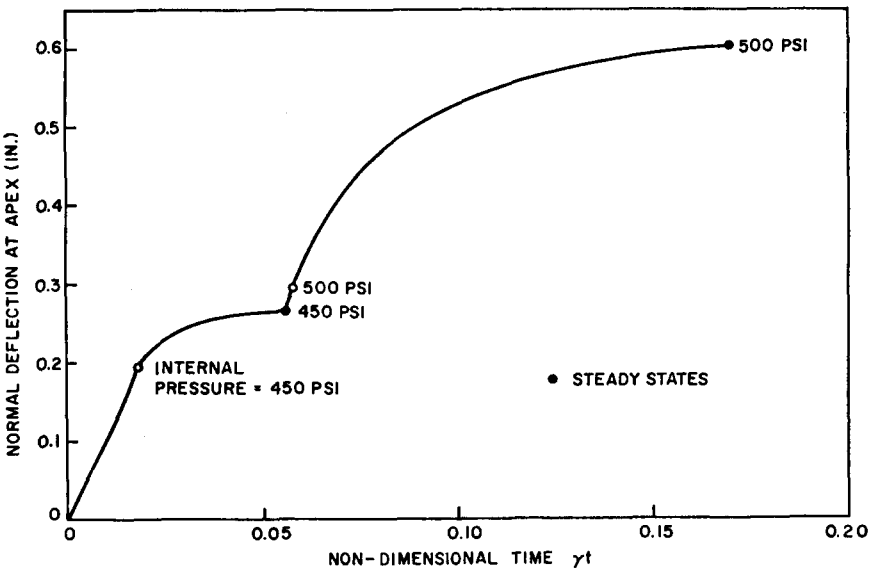

Fig. 7. Apex deflection vs. time—Elastic–plastic analysis of torispherical head using viscoplasticity formulation.

This pressure head was also analyzed for elastic–plastic behavior using the second method described in Section 4.3.1 in which time is used as an artifice in the viscoplasticity solution. The elastic–viscoplastic solution for $\gamma = 400$ sec.$^{-1}$ given in Fig. 5 was carried out until the internal pressure reached the value of 450 psi. Then the solution was allowed to progress with time towards a steady state elastic–plastic solution. Figure 7 shows the displacement–time curve reaching a steady state at about 0.265 in. and this is also indicated in the load–displacement graph in Fig. 6. The elastic–plastic solution of Section 7.1 is also plotted in this figure. The pressure was then increased to 500 psi using 10 psi increments in the viscoplastic analysis. Once again, displacement was allowed to increase with time in an artificial viscoplasticity solution. The solution reached a steady state at about 0.61 in., as can be seen from Fig. 7. It may be observed now that these steady state elastic–plastic displacements compare excellently with the results obtained by extrapolating for γ tending to infinity.

Comparing these results with the elastic-plastic solution taken from Section 7.1 it appears that this pressure vessel has an even softer behavior and lower collapse load than indicated by the extremely refined elastic–plastic solution. Hence, caution must be exercised before accepting such an analysis to have converged if the results therefrom are to be used for design purposes.

This example clearly demonstrates the capability of the viscoplastic analysis program to arrive at elastic–plastic solutions. The approach using a large value of γ in the viscoplastic analysis appears to be more economical than the other in which stress redistribution leads to steady states. This is due to the well known disadvantage of the initial strain formulation which requires the latter scheme to use a large number of pseudo-time steps or iterations, especially as the stiffness becomes very small. In the present example, both approaches, however, required about the same amount of computer time because four analyses (using different γ parameters) were used for the extrapolation technique. In contrast to these

methods, the direct analysis using the theory of plasticity required substantially less computing effort. Nevertheless, in the case of important and sensitive structures, it is desirable to have independent alternate methods which may be used to verify the accuracy and reliability of any particular analysis. Furthermore, the viscoplasticity approaches might be rendered competitive if automatic stepping techniques[13] are implemented to find the optimal time increment to be used at any time.

Acknowledgements—This work was partially supported by contracts DAAA21-72-C-0727 and -0729 with Mr. George Demitrack providing much encouragement. The computer facilities were provided by the Computer Center at the University of California, Berkeley.

REFERENCES

1. P. V. Marcal, Finite element analysis of combined problems of nonlinear material and geometric behavior, Technical Report No. N00014-0007/1, Brown University, Providence, R. I. (1969).
2. S. Yaghmai, Incremental analysis of large deformations in mechanics of solids with application to axisymmetric shells of revolution, Ph.D. Dissertation, University of California, Berkeley (1968), NASA, CR-1350 (1969).
3. L. D. Hofmeister, G. A. Greenbaum and D. A. Evensen, Large strain, elasto-plastic finite element analysis. *AIAA Journal*, **9**, 1248 (1971).
4. P. K. Larsen, Large displacement analysis of shells of revolution including creep, plasticity and viscoelasticity, Ph.D. Dissertation, University of California, Berkeley, SESM Report No. 71-22 (1971).
5. P. Perzyna, The study of the dynamic behavior of rate sensitive plastic materials, *Arch. Mech. Stos.* **15**, 113 (1963).
6. U. S. Lindholm, Dynamic deformation of metals. *Behavior of Materials Under Dynamic Loading*, edited by N. J. Huffington, Jr., ASME, New York (1965).
7. N. Cristescu, *Dynamic Plasticity*. North Holland Press, Amsterdam (1967).
8. U. S. Lindholm, Some experiments in dynamic plasticity under combined stress, *Mechanical Behavior of Materials Under Dynamic Loads*, edited by U. S. Lindholm. Springer, New York (1968).
9. C. H. Karnes, The plate impact configuration for determining mechanical properties of materials at high strain rates, *Mechanical Behavior of Materials Under Dynamic Loads*, edited by U. S. Lindholm, Springer, New York (1968).
10. F. E. Hauser, J. A. Simmons and J. E. Dorn, Strain rate effects in plastic wave propagation, *Response of Metals to High Velocity Deformation*, edited by P. G. Shewmon and V. F. Zackay, Interscience Publishers (1960).
11. F. E. Hauser, Techniques for measuring stress-strain relations at high strain rates, *Experimental Mechanics* **6**, 395 (1966).
12. J. Duffy, R. H. Hawley and R. A. Frantz, Jr., The deformation of lead in torsion at high strain rates, *J. appl. Mech.* **39**, 651 (1972).
13. O. C. Zienkiewicz and I. C. Cormeau, Visco-Plasticity solution by finite element process. *Arch. Mech. Stos.* **24**, 873 (1972).
14. J. T. Oden, Finite element formulation of problems of finite deformation and irreversible thermodynamics of nonlinear continua—A survey and extension of recent developments. Japan-U.S. Seminar on Mathematical Methods of Structural Analysis and Design, Tokyo (1969).
15. H. D. Hibbit, P. V. Marcal and J. R. Rice, A finite element formulation for problems of large strain and large displacements, *Int. J. Solids Struct.* **6**, 1069 (1970).
16. P. K. Larsen and E. P. Popov, Large displacement analysis of viscoelastic shells of revolution, *Comp. Meth. Appl. Mech. and Engng.* (in press).
17. J. T. Oden, *Finite Elements of Nonlinear Continua*. McGraw-Hill (1972).
18. J. T. Oden and J. E. Key, Numerical analysis of finite axisymmetric deformations of incompressible elastic solids of revolution, *Int. J. Solids Struct.* **6**, 497 (1970).
19. P. K. Larsen and E. P. Popov, A note on incremental equilibrium equations and approximate constitutive relations in large inelastic deformations, *Acta Mechanica* (in press).
20. M. Khojasteh-Bakht, Analysis of elastic-plastic shells of revolution under axisymmetric loading by the finite element method. Ph.D. Dissertation, University of California, Berkeley, Report No. SESM 67-8 (1967).
21. L. E. Malvern, The propagation of longitudinal waves of plastic deformation in a bar of material exhibiting a strain-rate effect, *J. Appl. Mech.* **18**, 203 (1951).
22. J. Lubliner, A generalized theory of strain-rate-dependent plastic wave propagation in bars, *J. Mech. and Phys. of Solids* **12**, 59 (1964).

23. V. V. Sokolovsky, Propagation of elastic–viscoplastic waves in bars, *Prik. Mat. Mekh.* **12**, 261 (1948). (In Russian.)
24. T. Von Karman and P. Duwez, Propagation of plastic deformations in solids, *J. Appl. Phys.* **21**, 987 (1950).
25. K. A. Rakhmatulin, On propagation of wave of unloading *Prik. Mat. Mekh.* **9**, 91 (1945). (In Russian.)
26. G. I. Taylor, The plastic wave in a wire extended by an impact load, *The Scientific Papers of G. I. Taylor*, edited by G. K. Batchelor, Vol. I. Cambridge University Press (1958).
27. P. Perzyna, The constitutive equations for rate sensitive plastic materials, *Quart. Appl. Math.* **20**, 321 (1963).
28. K. Hohenemeser and W. Prager, Über die Ansätze der Mechanik isotroper Kontinua, *ZAAM* **12**, 216 (1932).
29. P. Perzyna and W. Wojno, On the constitutive equations of elastic–viscoplastic materials at finite strain, *Arch. Mech. Stos.* **18**, 85 (1966).
30. T. Wierzbicki, Large deflections of a strain rate sensitive plate loaded impulsively, *Arch. Mech. Stos.* **21**, 67 (1969).
31. C. A. Calder, J. M. Kelly and W. Goldsmith, Projectile impact on an infinite viscoplastic plate, *Int. J. Solids Struct.* **7**, 1143 (1971).
32. P. Perzyna, Fundamental problems in viscoplasticity, from *Recent Advances in Applied Mechanics*. Academic Press, New York (1966).
33. S. Ahmad, B. M. Irons and O. C. Zienkiewicz, Curved thick shell and membrane elements with particular reference to axisymmetric problems, *Proc. 2nd Conf. on Matrix Methods in Structural Mechanics*, AFFDL-TR-68-150 (1968).
34. S. F. Pawsey, The analysis of moderately thick to thin shells by the finite element method, Report No. UCSESM 70-12. University of California, Berkeley (1970).
35. O. C. Zienkiewicz, R. L. Taylor and J. M. Too, Reduced integration technique in general analysis of plates and shells. *Int. J. for Num. Methods in Engng.* **3**, 275 (1971).
36. S. Nagarajan, Nonlinear static and dynamic analysis of shells of revolution under axisymmetric loading, Ph.D. Dissertation, University of California, Berkeley, SESM Report No. 73-11 (1973).

Абстракт — В первый раз дается общая формулировка анализа больших деформаций для пластических и вязкопластических задач. Определяются уравнения равновесия из вариационной формулировки приращения, на основе способа Лагранжа описания движения. Во всех конститутивных зависимостях применяются симметрическое напряжение Пиоля-Кирхгоффа и деформация Лагранжа. Путем использования вырожденных изопараметрических элементов, которые дают возможность реляксации гипозы Кирхгоффа-Лава, специализируется процесс расчета для анализа конечного элемента оболочек вращения, подверженных действию осесимметрической нагрузки. Для решения линеаризованных уравнений равновесия для приращения применяется преобразованный метод приращения, который использует исправление равновесия для каждого шага. Даются два подходы к решению для приспособления формулировки в рамках вязкопластичности, с целью использования невязких решений теории пластичности; один, заключающий в себя экстраполяцию результатов, когда коэффициент вязкости стремится к бесконечности и другой, в котором получаются решения для пластичности, применяя время как изобретение в анализе вязкопластичности, пока достигаются состояния равновесия для каждого поступательного уровня нагрузки. Представляется подробное исследование нелинейного поведения торосферического сосуда давления, с целью иллюстрации эффективности численных методов.